IMPROVING ORBIT DETERMINATION FOR GEOSTATIONARY SATELLITES VIA. DATA FUSION

Joseph chan(1), Hideshi Chazono(2), Taku Izumiyama(3)

(1)Intelsat Corporation, 3400 International Dr., NW, Washington DC, 2008
Joseph.chan@intelsat.com
(2,3)Sky Perfect JSAT Corporation, 229-1 Miho-cho, Midori-ku, Yokohama 226-0015, JAPAN
chazono-hideshi@sptvjsat.com
(3,2)IHI Corporation, 900, Fujiki, Tomioka-shi, Gunma, 370-2398 JAPAN
taku_izumiyama@ihi.co.jp

ABSTRACT

Intelsat Ltd. (IS), SKY Perfect JSAT Corporation (SJC) and IHI Corporation (IHI) conducted a joint study to evaluate accuracies and error covariance of determined orbits for IS and SJC satellites by using solo optical observed data from IHI optical observation demonstrator, and combined data from tradition ranging data. Optical data has proven to be very useful for space surveillance and close approach monitoring providing improved orbital knowledge of both active and non-active space objects. As satellite operators we are also interested in using optical data to complement our standard ranging measurements to improve our orbit uncertainties and help to resolve and calibrate sensor biases. In the first phase of our join study IHI provided optical observations for both IS and SJC satellites and we will present the multi-objectives of our join study and preliminary results in the orbit comparisons and error estimations from different fusion techniques.

1 BACKGROUND OF JOINT STUDY

IHI Corporation, SKY Perfect JSAT and Intelsat agreed to work together on a joint study in late 2012 to study the feasibility of using optical data to improve satellite operations with the following objectives: (1) to evaluate the use of optical data to resolve un-known measurement range biases in an un-calibrated range antenna, (2) to evaluate the different data fusion techniques and the improvement to orbit determination and orbit error estimates by fusing optical data with ranging data and (3) to evaluate the feasibility of using optical data to refine the relative distances between two closely located satellite to improve conjunction monitoring and safe operations in close proximity operations.

2 OPTICAL DATA PROCESSING

For optical observation on geostationary satellites, IHI Orbital Object Optical Observation Demonstrator (IO4D) was used. IO4D was developed by IHI as a demonstrator for research on orbiting objects observation technologies and data analysis processes using small telescope but effectively.

IO4D consists of four major elements; a telescope with equatorial mounting, a 16M pixel cooled charge-coupled device (CCD) camera, GPS time stamp and a controller with data processing capability. Aperture of the telescope is 20-cm and its focal length is 800m. Total sky coverage of the image area of the system is around 2.58 degrees by 1.72 degrees, and its pixel scale is about 1.9 arc second. The start and end time of exposure are recorded in the image header using global positioning system (GPS) time recorder.

IO4D is not fixed but mobile equipment, so IHI selected Test Area of IHI Aerospace Tomioka Works, which is located approximately in the center of Japan, as the suitable location for the purpose of observation.

IHI Aerospace Co., Ltd. is one of IHI subsidiaries and it becomes enough dark to observation at night in the Test Area.

Equipment setting was conducted every evening and packed up during daytime. Therefore, observation point is changed a little bit for each observation night and the position was measured by GPS receiver every day. Typical number of the position is at 138.933860 deg E, 36.301501 deg N, 208.6m altitude in WGS 84. There places of decimals for longitude and latitude may vary on each day.

All images were taken while motion of the equatorial was stopped. After short exposure, long exposed images were taken to detect geostationary satellites. Images processing techniques were applied to obtain positions of target satellites from images taken through observation. After correction of noise and photographic sensitivity of images, positions (x, y) of stars in each image in short exposure were analysed. Through comparison of star positions in each image with positions shown in star catalogue, stars in the images were identified and right ascension (α) and declination (δ) of center of each image, which is the same as bore sight direction of the telescope, were calculated. Then transfer matrix from x-y coordination system in the image to α-δ equatorial coordination system as function of time was calculated. Hubble Guide Star Catalog – Astrographic Catalog / Tycho (GSC-AST) was used for

Proc. '6th European Conference on Space Debris'
Darmstadt, Germany, 22–25 April 2013 (ESA SP-723, August 2013)

identification of stars. The centers of long exposed images were calculated to shift right ascension to time since time of images in short exposure. Positions (x, y) of satellites in long exposed images were analyzed and converted into equatorial coordination system by the transfer matrix. Satellite positions in J2000.0 were obtained.

3 OPTICAL OBSERVATIONS

Two sets of observations were taken in November 15-16, 2012 and March 14-17, 2013. The measurements were taken on 8 satellites. The summary of the observation activities is shown in Tab. 1.

	JSAT 4A	JSAT 13	JSAT 5A	JSAT 3A	JSAT 12	IS701	IS706	IS8	IS19
Long (E)	124	124	132	128	128	157	157	169	166
15-Nov	x	x	x	x	x	x		x	x
16-Nov	x	x	x	x	x	x		x	x
14-Mar		x	x	x	x			x	x
15-Mar		x	x	x	x		x	x	x
16-Mar		x	x	x	x		x	x	x
17-Mar		x	x	x	x		x	x	x

Table 1, the optical data observation summary

IHI has identified some processing errors for the data taken in Nov 2012 and is re-processing the images to correct the errors.

Preliminary results of the data for IS701, IS8 and IS19 before the re-processing are shown in Fig. 1 to Fig. 3.

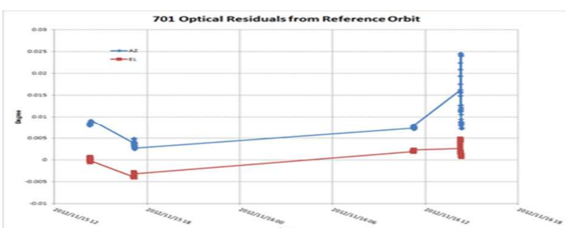

Figure 1, Data residuals for IS701 based on reference solution using 2 station ranging data

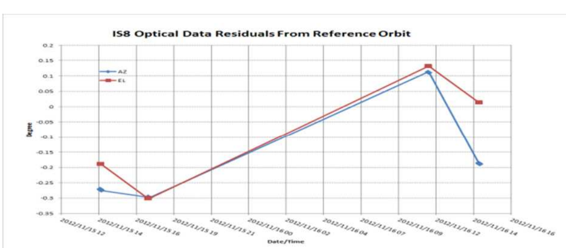

Figure 2, Data residuals for IS8 based on reference solution using 2 station ranging data

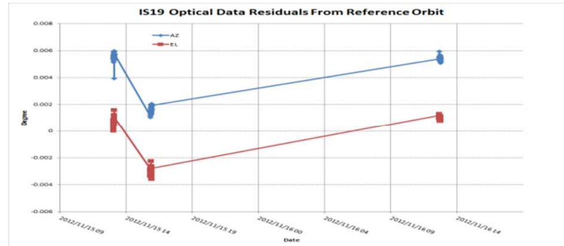

Figure 3, Data residuals for IS19 based on reference solution using 2 station ranging data.

Optical data only solutions were computed and compared against the reference solutions using two station ranging data. The results of the comparisons are shown in Tab. 2.

IS19 Optical Only

--PARAMETER--		---FINAL VALUE----	--REFERENCE VALUE--	-----DELTA----	
X-position	:	39005.2849205134	38994.6060742489	10.6787462646	km
Y-position	:	-16040.9313106230	-16039.5936973413	-1.3376132818	km
Z-position	:	-4.8611946978	-7.1973600762	2.3361653783	km
X-velocity	:	1.1689811997	1.1699780267	-0.0009968270	km/s
Y-velocity	:	2.8430051055	2.8433733708	-0.0003682653	km/s
Z-velocity	:	0.0014936556	0.0015750353	-0.0000813797	km/s

IS8 Optical only

--PARAMETER--		---FINAL VALUE----	--REFERENCE VALUE--	-----DELTA----	
X-position	:	-17447.6080064759	-18058.3548967593	610.7468902833	km
Y-position	:	-38525.0266818355	-38092.3487883359	-432.6778934996	km
Z-position	:	-46.9302302776	-7.5058502258	-39.4243800518	km
X-velocity	:	2.7951063483	2.7788865739	0.0162197744	km/s
Y-velocity	:	-1.2599803851	-1.3177430326	0.0577626475	km/s
Z-velocity	:	0.0080357037	0.0022304869	0.0058052168	km/s

IS701 Optical only

--PARAMETER--		---FINAL VALUE----	--REFERENCE VALUE--	-----DELTA----	
X-position	:	21751.7912814966	21762.5029914402	-10.7117099436	km
Y-position	:	36138.4192563241	36131.3190795179	7.1001768062	km
Z-position	:	-185.6679095613	-184.5068595239	-1.1610500374	km
X-velocity	:	-2.6332610329	-2.6326152583	-0.0006457747	km/s
Y-velocity	:	1.5845870601	1.5857156136	-0.0011286444	km/s
Z-velocity	:	0.0399026132	0.0400166893	-0.0001140740	km/s

Table 2, Comparisons of optical data only solutions with corresponding reference solutions using two station ranging.

The results showed that there is about 15 km RSS position differences from the reference solutions for IS701 and IS19. The large difference with IS8 is expected due to the large residuals. The observed differences should be reduced after IHI re-processed the Nov 2012 data which they have identified some errors in the original processing.

JSAT has processed a set of the more recent observations taken in March 2013 on JSAT5A. The preliminary is showing very good results with the improved image processing steps.

The measurement residuals as well as orbit differences are shown below.

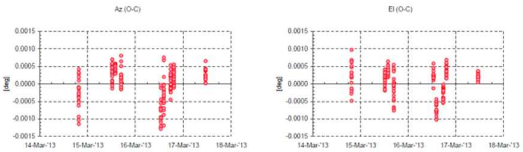

Figure 4, JSAT 5A optical measurement residuals from reference solution using two station ranging.

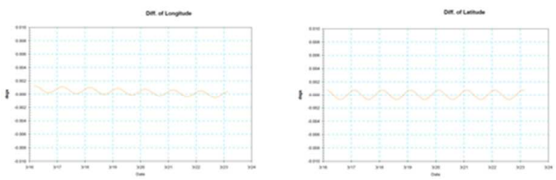

Figure 5, JSAT 5A latitude and longitude differences between the optical only solution and the reference solution using two station ranging.

4 RANGE MEASUREMENT BIAS CALUBRATION

One of the goals in this joint study is to evaluate the use of optical data to calibrate sensor measurement biases. We have combined the two station ranging solution with optical data and solve for the two range measurement biases simultaneously in a single solution. The results for IS19 are shown in Tab. 3a and Tab. 3b. Tab. 3a shows the solution with optical data added to the range data. A change of about 150 meter in the bias and 2 km RSS change in the orbit position from the reference solution was observed with the new solved for biases. Tab 3b shows the simultaneous solutions solving for two measurement biases using only two station ranging. The results indicated a highly correlated solution this is expected due to the collinearity of the two measurement biases in the normal equations.

--PARAMETER--		---FINAL VALUE----	--REFERENCE VALUE--	-----DELTA-
KSN-K22 range bias	:	-5.4944859818	0.0067837700	-5.50126975
NAP-K31 range bias	:	6.8956888203	-0.7324297139	7.62811853
X-position	:	39019.4788506179	38994.4364067689	25.04244384
Y-position	:	-15978.9474791739	-16039.9782883992	61.03080922
Z-position	:	-7.0878999405	-7.0883745995	0.00047465
X-velocity	:	1.1655551317	1.1700054220	-0.00445029
Y-velocity	:	2.8451903582	2.8433623562	0.00182800
Z-velocity	:	0.0015595993	0.0015690631	-0.00000946

Table 3a, IS19 range measurement bias solution with optical data

--PARAMETER--		---FINAL VALUE----	--REFERENCE VALUE--	-----DELTA----
KSN-K22 range bias	:	0.1602991313	0.0067837700	0.1535153613
NAP-K31 range bias	:	-0.9484344607	-0.7324297139	-0.2160047468
X-position	:	38993.7581850515	38994.4364067689	-0.6782217174
Y-position	:	-16041.6766351051	-16039.9782883992	-1.6983467059
Z-position	:	-6.7296279092	-7.0883745995	0.3587466903
X-velocity	:	1.1701215057	1.1700054220	0.0001160837
Y-velocity	:	2.8433133382	2.8433623562	-0.0000490179
Z-velocity	:	0.0014880827	0.0015690631	-0.0000809804

Table 3b, IS19 range measurement bias solution using two station ranging only

In Tab. 4 we show the measurement bias solutions for IS701 with different data weight used for the optical data. In these cases the results indicated that depending on the data weight used for the optical data the final solutions could vary quite a lot.

- Medium Weight:

--PARAMETER--		---FINAL VALUE----	--REFERENCE VALUE--	-----DELTA----	
KSNC21 range bias	:	0.2483812178	0.0000000000	0.2483812178	km
PAM-C05 range bias	:	-0.4400553625	0.0000000000	-0.4400553625	km
X-position	:	21765.5616621193	21762.5029914402	3.0586706791	km
Y-position	:	36129.4361988005	36131.3190795179	-1.8828807174	km
Z-position	:	-184.9239959322	-184.5068595239	-0.4171364083	km
X-velocity	:	-2.6325010853	-2.6326352583	0.0001341730	km/s
Y-velocity	:	1.5859436288	1.5857166136	0.0002270152	km/s
Z-velocity	:	0.0400364569	0.0400166893	0.0000197677	km/s

- High Weight:

--PARAMETER--		---FINAL VALUE----	--REFERENCE VALUE--	-----DELTA----	
KSNC21 range bias	:	-0.4128039826	0.0000000000	-0.4128039826	km
PAM-C05 range bias	:	0.1710607237	0.0000000000	0.1710607237	km
X-position	:	21756.6927661522	21762.5029914402	-5.8102252880	km
Y-position	:	36134.8579734712	36131.3190795179	3.5388939533	km
Z-position	:	-185.5676947492	-184.5068595239	-1.0608352253	km
X-velocity	:	-2.6330433109	-2.6326352583	-0.0004080527	km/s
Y-velocity	:	1.5850497261	1.5857166136	-0.0006668874	km/s
Z-velocity	:	0.0398937576	0.0400166893	-0.0001229316	km/s

- Low Weight:

--PARAMETER--		---FINAL VALUE----	--REFERENCE VALUE--	-----DELTA----	
KSNC21 range bias	:	5.4175829926	0.0000000000	5.4175829926	km
PAM-C05 range bias	:	-8.9100514305	0.0000000000	-8.9100514305	km
X-position	:	21832.0408486321	21762.5029914402	69.5378571919	km
Y-position	:	36089.3239029205	36131.3190795179	-41.9951765974	km
Z-position	:	-184.5825156809	-184.5068595239	-0.0756561570	km
X-velocity	:	-2.6295787121	-2.6326352583	0.0030565462	km/s
Y-velocity	:	1.5907830966	1.5857166136	0.0050664830	km/s
Z-velocity	:	0.0399929133	0.0400166893	-0.0000237759	km/s

Table 4, IS701 measurement bias solutions with using two station ranging and optical data with different data weight for the optical data. The differences are from the reference solution using two station ranging.

Based on the above results it is important to determine the proper data weight one should apply to the optical data when developing combination solutions.

5 DATA FUSION

In Tab. 5 we compared two orbit solutions using IS8 using single station ranging only solution and a combination solution with single station ranging and optical data. The differences are from a reference solution using two station ranging. It is interesting to note that the single ranging solutions shows over 60 km RSS in orbit position differences but the combination solution using both single station ranging and optical data shows less than 5 km RSS in orbit position. Please note that Fig. 2 showed very large residuals for the IS8 optical data. The results in Tab.5 demonstrated that by combing range and optical data one can greatly improves the final combined solution results even if either data type when used individually gives "poor" results. The important consideration is that the data weights are applied appropriately. We have shown that even "poor" can be used to improve solutions if the data are properly characterized by the data weight used in the fused solutions.

IS8 solution using single station ranging only

--PARAMETER--		---FINAL VALUE----	--REFERENCE VALUE--	-----DELTA----	
X-position	:	-18070.7702947916	-18060.8548967593	-9.9153980323	km
Y-position	:	-38082.3343363068	-38092.3497983359	10.0154620291	km
Z-position	:	49.8436464211	-7.5053502258	57.3489966469	km
X-velocity	:	2.7787202791	2.7785865738	0.0001337053	km
Y-velocity	:	-1.3182551153	-1.3177430326	-0.0005120828	km
Z-velocity	:	0.0077366238	0.0022304889	0.0055061349	km

IS8 single station ranging and optical data

--PARAMETER--		---FINAL VALUE----	--REFERENCE VALUE--	-----DELTA----	
X-position	:	-18065.5857528203	-18060.8548967593	-4.7308560610	km
Y-position	:	-38090.5534683622	-38092.3497983359	1.7963299737	km
Z-position	:	-8.1130589591	-7.5053502258	-0.6077087333	km
X-velocity	:	2.7785173534	2.7785865738	-0.0000692204	km
Y-velocity	:	-1.3178155195	-1.3182551153	0.0004395958	km
Z-velocity	:	0.0051235060	0.0022304889	0.0028930171	km

Table 5, IS8 solutions using single station ranging and optical data

Based on the discussions above it is interesting to determine what the optimal data weights should be when considering data fusion. We will propose a technique based on the subset solution which was used for the development of GEM gravity models by Lerch[1]. The general idea of this technique is to select a data weights for the different data type so that the differences of the subset solution and the combined solution "equals" to the expected values of the differences, i.e.,

$$(X_t - X)^T (X_t - X) \approx tr[E(X_t - X)(X_t - X)^T]$$

The implied consequence for this technique is an optimal data weight of the subset data and thus a realistic the covariance estimate of the combined solution. This realistic covariance can be used to characterized the orbit solution which can then be used to produce a realistic collision probability for decision making in close approach situations.

We will derive this data weight calibration technique following the outline in the paper by Lerch[2].

Consider the following observation equation for each data type t:

$$r_t = A_t x + n_t$$

Where:

$$r_t = residuals \;\; from \; reference \; solution: \; O - C_R$$
$$n_t = measurment \;\; noise$$
$$A_t = observation \; matrix$$

Defining:

$$N_t \equiv A_t^T A_t \qquad R_t \equiv A_t^T r_t$$

The normal matrix for the subset and combined solutions can be written as:

$$\bar{N} = \sum_{j \neq t} w_j N_j \qquad \bar{R} = \sum_{j \neq t} w_j R_j$$

$$N = \bar{N} + w_t N_t \qquad R = \bar{R} + w_t R_t$$

We can write the orbit solutions as:

$$N\, x = R$$
$$\bar{N}\, x_t = \bar{R}$$

Where:

$$x = X - X_R \qquad x_t = X_t - X_R$$

X_R is the reference solution

X is the combined solution with all the data type included

X_t is the subset solution with data type removed

In order to complete the calibration we need to calculate

$$E(X_t - X)(X_t - X)^T = E(x_t - x)(x_t - x)^T$$
$$= V(x_t - x)$$

Consider the following covariance:

$$V(x) = N^{-1} = E(xx^T)$$
$$V(x_t) = \bar{N}^{-1} = E(x_t x_t^T)$$

We will show that under the assumption that the errors of different type are independent, i.e.,

$$E(\bar{R} R_t^T) = 0$$

Then:

$$V(x_t - x) = V(x_t) - V(x)$$

Consider the following:

$$
\begin{aligned}
V(x_t - x) &= E(x_t - x)(x_t - x)^T \\
&= V(x_t) - 2E(x_t x^T) + V(x)
\end{aligned}
$$

$$
E(x_t x^T) = \bar{N}^{-1} E(\bar{R} R^T) N^{-1}
$$

$$
\begin{aligned}
E(\bar{R} R^T) &= E(\bar{R}(\bar{R} + w_t R_t)^T) \\
&= E(\bar{R}\bar{R}^T) + w_t E(\bar{R} R_t^T) \\
&= \bar{N} + w_t E(\bar{R} R_t^T)
\end{aligned}
$$

For a calibrated solution with optimal data weight we write:

$$
\begin{aligned}
(X_t - X)^T (X_t - X) &= k_t \, tr[E(X_t - X)(X_t - X)^T] \\
&= k_t \, tr[V(x_t - x)] \\
&= k_t \, tr[V(x_t) - V(x)]
\end{aligned}
$$

Where for calibrated solution: $k_t = 1$

6 AN EXMAPLE WITH IS19

In order to illustrate this technique we will conduct an experiment using IS19. We will create the following solutions:

(1) "Truth" reference solution using two station ranging data for the entire 3 day span.
(2) "Baseline" solution using only single station ranging data for 1 day span
(3) "Fused" solutions by combing the single station range data with optical data with different data weights

--PARAMETER--		---FINAL VALUE----	--REFERENCE VALUE--	-----DELTA----	
Semi-major axis	:	42165.2913906099	42165.2820240959	0.0093665139	km
Eccentricity	:	0.0002242127	0.0001263093	0.0000979034	
Inclination	:	0.0859089382	0.0306580763	0.0552508618	degree
RA of Asc Node	:	320.1175480763	356.0379684472	-35.9204203709	degree
Arg of perigee	:	280.6025753525	259.8751992437	20.7273761089	degree
True Anomaly	:	96.9328718844	81.7277357682	15.2051361162	degree
X-position	:	38999.6425256539	38994.4960811409	5.1464445131	km
Y-position	:	-16032.3229030409	-16039.8116530392	7.4887499983	km
Z-position	:	19.0491429737	-7.1204418514	26.1695848251	km
X-velocity	:	1.1696157370	1.1699934279	-0.0003776909	km/s
Y-velocity	:	2.8433698582	2.8433680936	0.0000017646	km/s
Z-velocity	:	0.0043960273	0.0013610627	0.0028349647	km/s
Drift	:	0.0065133264	0.0066332732	-0.0001199467	deg/re
Longitude	:	166.0334252883	166.0213543940	0.0120708943	degree

Table 6, Orbit difference of the "baseline" solution with the "truth".

We generated different sample fused solutions by adjusting the data weight of the optical data and compute the calibration factor k.

1/w (deg)	K
0.003	0.86
0.005	0.87
0.01	0.91
0.02	1.01
0.025	1.06
0.05	1.37
0.1	2.53

Table 7, Calibration factor k as a function of data weight for the IS19 example.

As shown above for k < 1 implies that the change in the orbit solution with and with the data type is smaller than the change in the covariance of the two solutions indicating the data weight is too high. For k > 1 implies that the change in the orbit solutions with and without the data type is larger than the change in the covariance of the two solutions indicating the data weight is too low. An optimal data weight is indicated when k = 1.

Based on Tab. 7 the optimal data weight (1/w) is 0.02 degree. The optimal solution differences from the "truth" are given below.

--PARAMETER--		---FINAL VALUE----	--REFERENCE VALUE--	-----DELTA----	
Semi-major axis	:	42165.3018127175	42165.2820240959	0.0197886216	km
Eccentricity	:	0.0001229254	0.0001263093	-0.0000033839	
Inclination	:	0.0278838392	0.0306580763	-0.0027742372	degrees
RA of Asc Node	:	349.3343906900	356.0379684472	-6.7035777572	degrees
Arg of perigee	:	262.6805486722	259.8751992437	2.8053494286	degrees
True Anomaly	:	85.6261900134	81.7277357682	3.8984542452	degrees
X-position	:	38994.9207986902	38994.4960811409	0.4247175493	km
Y-position	:	-16039.8074660721	-16039.8116530392	0.0041869671	km
Z-position	:	-4.1588674306	-7.1204418514	2.9615744208	km
X-velocity	:	1.1699647106	1.1699934279	-0.0000287173	km/s
Y-velocity	:	2.8433499264	2.8433680936	-0.0000181672	km/s
Z-velocity	:	0.0014652319	0.0013610627	-0.0000958308	km/s
Drift	:	0.0063798617	0.0066332732	-0.0002534114	deg/rev
Longitude	:	166.0215793009	166.0213543940	0.0002249069	degrees

Table 8, Optimal fused solution differences from the reference solution using two station ranging.

Comparing Tab 6 and Tab. 8 we observed great improvements when optical data are added to the "baseline" solution using only single station ranging data.

Results comparing the differences over the data span are shown in figures below:

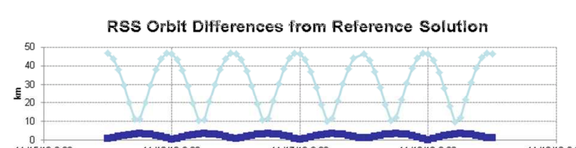

Figure 6, IS19 RSS orbit differences from reference two station ranging solution over 3 day span

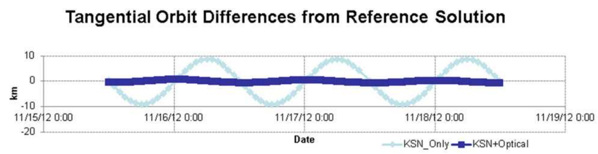

Figure 7, IS19 Tangential orbit differences from reference two station ranging solution over 3 day span

The results from above figures are consistent with the results displayed in Tab. 8 that the optical data significantly improved the orbit solution using only single station ranging data over the 3 day span. Note that the solutions are computed with only 1 day of data.

One other criterion for the optimal solution is to obtain a realistic covariance. We computed the error estimates of the combined solution and compared that with the actual differences with the reference solution, the "Truth" in this experiment.

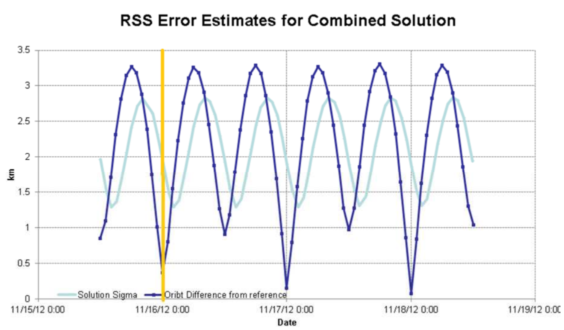

Figure 8, comparing the orbit differences with the predicted orbit error.

Note that we have only about one day of optical data and in the figure above the comparisons to the right of the yellow line are predictions outside of the data span. We noticed that the absolute error estimate seemed to optimistic and it is also interesting to notice that there seemed to be a phase offset between the error estimates and the orbit differences. This implies the data weight may be too high.

There are a few limitations to the current implementation to the subset solution calibration technique. We applied the calibration using only the orbit position components at the solution epoch. We are considering modifying the implementation to include sample data points within the data span and to consider also the velocity components when computing the calibration factor k described above.

7 CONCLUSION AND FUTURE PLANS

IHI has completed two sessions of optical observations using IHI mobile telescope in Nov, 2012 and March 2013. Based on preliminary results the data are providing good results. IHI has identified an improvement to the process the images for the 1st session of the telescope observations and are working to re-process the data. We have demonstrated that the optical data provide much improvement to calibrate the range measurement biases if the optical data are weighted properly. We have proposed two criteria for determining optimal data weights: (1) improved solutions and (2) realistic covariance. Having a realistic covariance is very important. One application from having a realistic covariance with the orbit solution is to provide realistic conjunction probability to help with decisions on potential close approaches. We have demonstrated the feasibility to use the subset solution technique to determine the optimal data weight. The results showed encouraging results but also some limitations in our implementation of the technique. We will continue to experiment this technique with the 2nd sessions of the telescope data and the re-processed data from the 1st session. IHI is also planning to build another permanent telescope site about 400 km from this current mobile site. The plan is to have it ready for observation by end of 2013. It will be add strength to the optical data.

IHI has also taken optical data with both satellites (JSAT3A/JSAT12) in the same FOV to provide the data to study the concept of using optical data to assist conjunction monitoring for close approach objects. It was also discussed by chan[3] and the idea is that if a potential conjunction involves an active satellite and a non-active space debris one will try to solve for the orbit solution of the non-active satellites using the relative angles data from the image with both satellites in the same FOV. Fig. 9 and 10 describes the scenario.

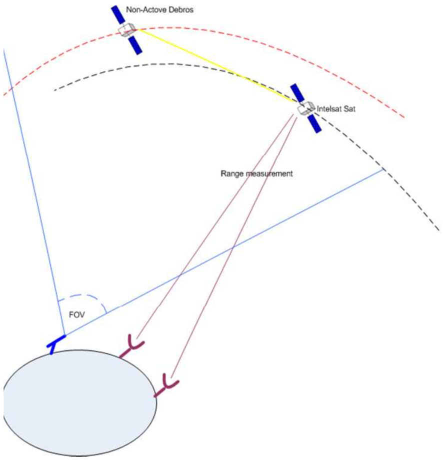

Figure 9, describing the concept of computing the orbit of the non-active object using relative angles form the active satellite which is also tracked with two station ranging.

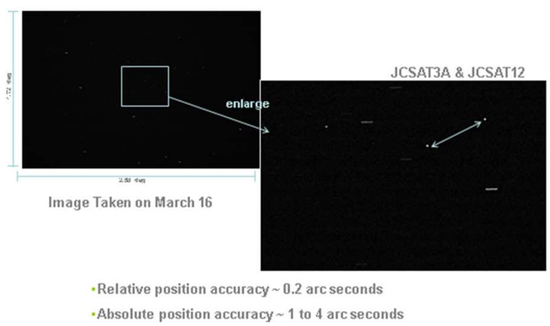

Figure 10, showing the improvement to the uncertainties when using relative angles for orbit determination

The improvement for this approach is due to the great reduction in the uncertainties of the relative motion of the two satellites. As shown in Fig. 10 the relative position accuracy for relative angels on the image is about 0.2 arcseconds while the position accuracy for absolute position ranges from 1 to 4 arcseconds. Using this approach we will improve the relative orbit differences between the two satellites enabling precise decision making concerning this close approach encounter.

REFERENCES

1. "Lerch, F. J., Optimum data weighting and error calibration for estimation of gravitational parameters" Bull Geod., 65, 44-52, 1991
2. Lerch, F. J., et al., Gravity Model Development for Topex/Poseidon: Joint Gravity Models 1 and 2" JGR, vol. 99, no. C12, Dec 15, 1994
3. Chan, J., Intelsat Experiences on Satellite Conjunctions and Lesson Learnt, AAS 11-436, AAS/AIAA Astrodynamics Specialist Conference, July 31 – August 4.